Paper No. 771. (quote when citing this article)
Eleventh World Conference on Earthquake Engineering
ISBN: 0 08 042822 3

BEHAVIOUR OF A STEEL-CONCRETE COMPOSITE SUBSTRUCTURE WITH FULL AND PARTIAL SHEAR CONNECTION

O.S. Bursi and M. Ballerini
Department of Structural Mechanics, University of Trento,
Via Mesiano 77, 38050, Trento,Italy.

ABSTRACT

A method of analysis for steel-concrete composite structures subjected to cyclic lateral loads is proposed as part of an overall investigation of aseismic design of composite structural systems. In developing the method, quasi-static cyclic tests on composite beams with full and partial shear connection as well as complementary cyclic tests on pull-push specimens were performed. These tests are used both to expand the experimental data base and to calibrate finite element models. The paper presents significant results of the research to date.

KEYWORDS

Steel-concrete composite beam; partial shear connection; full shear connection; pull-push specimen; quasi-static cyclic test; pseudodynamic test; slab effective width.

BEAM-COLUMN SUBASSEMBLAGES

Composite framing systems consisting of steel-concrete composite beams, steel or composite columns and rigid or semi-rigid joints have been recognized to be a viable alternative to conventional reinforced concrete or steel framing systems. However, only limited studies (Bouwkamp and Fehling, 1992, Kim and Lu, 1994) were conducted to investigate the overall performance of such systems in earthquake prone zones. Furthermore, while extensive research was carried out to analyse the behaviour of composite beams with partial shear connection (PSC beams) under vertical loads, no hysteresis analytical models were available for PSC beams subjected to cyclic lateral loads, when the present research was initiated.

Test Subassemblages and Procedures

In order to expand the experimental data base and to calibrate finite element models for the improvement of code-formatted procedures for aseismic design, six composite beam specimens with full shear connection (FSC) and PSC indicated schematically in Fig. 1 were built. They represent a full scale model of half bay within a moment-resisting frame. These specimens are endowed with pins in the column midheight above and below the connection and at midspan of the beam as is commonly postulated for moment frames subjected to lateral loads. In the first phase of the research, the specific recommendations drafted by ECCS (1986) are applied on two companion FSC and PSC specimens, respectively. The geometrical characteristics as well as the details of the composite subassemblages are shown in Fig. 1. In order to confine the failure mechanisms at the composite beam, the column has an heavy HE 360 B section. Likewise, the beam-to-column joint is designed to be rigid and full strength. As a result, the beam section is welded to the column and additional rebars are located around the column as shown in Fig. 1b. Headed stud shear connectors are designed to fail by shearing thus avoiding brittle concrete-pullout failure. Both strength and ductility of connectors are enhanced by using larger

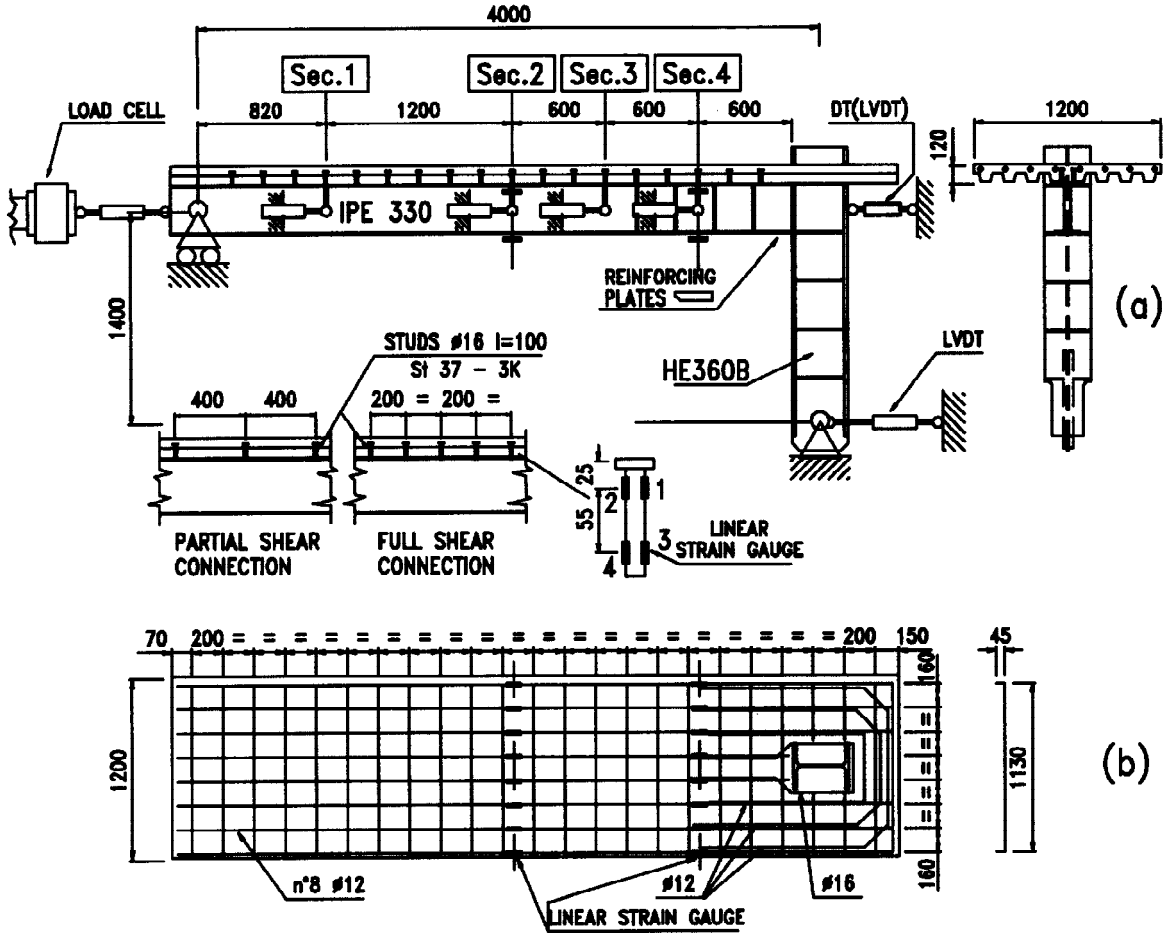

Fig. 1. Test substructure characteristics and measurement apparatus: (a) lateral views; (b) top view.

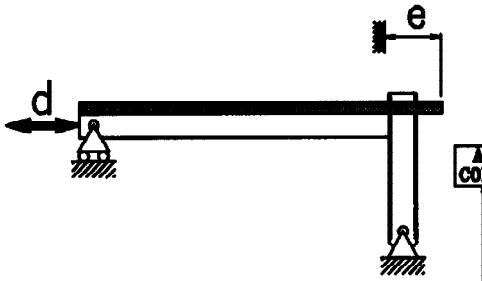

Fig. 2. Internal *d* and controlled *e* displacements.

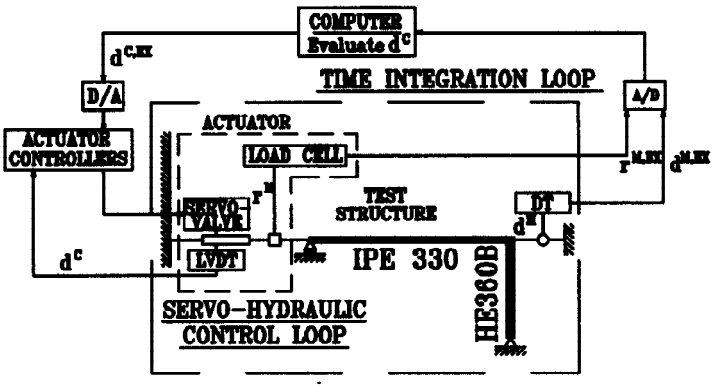

Fig. 3. Schematic of the pseudodynamic test setup.

stud spacings and ribs parallel to the direction of the applied shear (Hawkins and Mitchell, 1984).
One subassemblage specimen is shown schematically in Fig. 2 with the controlled displacement parameter e. By means of the ECCS short testing procedure (1986), stiffness, strength, ductility and absorption energy properties of each specimen can be determined. In addition, a comparative assessment of the specimen performances can be carried out. However, the major problem of testing structural systems with the conventional quasi-static cyclic approach consists in the uncertainty to relate the cyclic response to the seismic performance. Furthermore, the ECCS procedure seems to be quite severe for the assessment of ductility levels and may not allow the potential strength of the tested component to be fully achieved. As a result, pseudodynamic tests are going to be performed on other three companion specimens by means of the test setup shown in Fig. 3. This setup reproduces the scheme developed by Shing *et al.* (1991). As shown in Fig. 3, the integration procedure is implemented with a dual displacement control by using both an external digital displacement transducer and an internal analog transducer. This prevents the deformation of the reaction frame supporting the actuator from affecting the actual structural displacement, while avoiding any external disturbance to the transducer used in the servo-control loop.
The measurement apparatus is shown schematically in Fig. 1. It is composed of an analog transducer internal to the actuator and the relative load cell. Furthermore, reaction frame displacements as well as composite beam axial displacements can be detected by means of an external digital transducer (DT) at the steel beam centroid as well as one LVDT at the base, both shown in Fig. 1a. However, an external LVDT has been used for the first two composite beam tests. The slip between the steel beam and the composite slab is detected by means of coupled LVDTs shown in Fig. 1a, and located at Secs. 1-4. In order to detect beam flange strains as well as rebar axial deformations linear strain gauges are located at Secs. 2 and 4. Within these sections, each stud connector is instrumented with four strain gauges,labelled from 1 to 4, to capture the axial and bending deformation distribution. Based on actual material properties, a conventional degree of shear connection (Eurocode 4 (EC-4), 1992) F_c/F_{cf} equal to 1.36 and 0.68 has been computed for the FSC and PSC beams, respectively.

Test Results

According to the specific recommendations drafted by ECCS (1986), the horizontal displacement e (Fig. 2) is assumed to be the prime parameter of test control. In line with the short testing procedure (ECCS, 1986), the amplitude of initial cycles was selected small enough to detect the onset of yielding. Then, conventional elastic limit values, i.e. the displacement e_y and the force F_y were determined a posteriori on the force-displacement envelope relationships by means of best fitting. These values for positive as well as negative hemicycles are $e_y^+ = 15$, 17 mm, $F_y^+ = 252$, 248 kN and $e_y^- = -17.2$, -17.2 mm, $F_y^- = -210$, -210 kN for the FSC and PSC beams, respectively. One can observe that the aforementioned values are not symmetrical and that the PSC beam appears to be less strong and more ductile when compared to the FSC beam.
For conciseness, only main results are presented in what follows. The hysteresis loops of the reaction force developed by the FSC beam against the controlled displacement e (see Fig. 2) are plotted in Fig. 4. Hysteresis cycles appear to be stable. Furthermore, the inelastic hysteretic behaviour exhibited by the specimen is governed by steel beam yielding for positive (pull) loads and rebar yielding as well as concrete fracturing for negative (push) loads. Web and flange buckling occurred at the first negative hemicycle characterized by a partial ductility ratio $e/e_y^- = 4$. However during the test, positive as well as negative ductility levels $e/e_y = 6$ were reached. Collapse was governed by crushing and uplifting of the composite slab at Sec. 4 (see Fig. 1b). The reaction force value corresponding to the bending resistance at Sec. 4 predicted by EC-4 (1992) without partial safety factors for resistances and material properties is also indicated in Fig. 4. One can observe that EC-4 provides inaccurate plastic failure resistance values for specimens subjected to lateral loads. The corresponding reaction force-controlled displacement loops of the PSC beam are reported in Fig. 5. Also in this test hysteresis cycles appear to be stable. However, web and flange buckling revealed at the first hemicycle with $e/e_y^- = 4$. In addition, at the third positive hemicycle of the same set, weld beads between the beam bottom flange and the column fractured. In spite of this collapse mode, a negative hemicycle at a ductility ratio $e/e_y^- = 6$ was carried out, followed by a positive hemicycle at a ductility ratio $e/e_y^+ = 6$. Also in this case, the reaction force value corresponding to the bending resistance at Sec. 4 predicted by EC-4 (1992) can be compared to the measured values in Fig. 5. Even for this test EC-4 predictions appear to be unsatisfactory. The aforementioned preliminary results show that both specimens are able to reach partial ductility levels equal to 6, though the PSC specimen exhibited a large resistance drop. However, if these specimens are assumed to be part of a framing system with an interstorey height $h = 3500$ mm, it appears that the the ratio $2(6e_y^-)/h$ is well beyond 2.5 % which represents a practical limit over which the framing system has to be demolished.

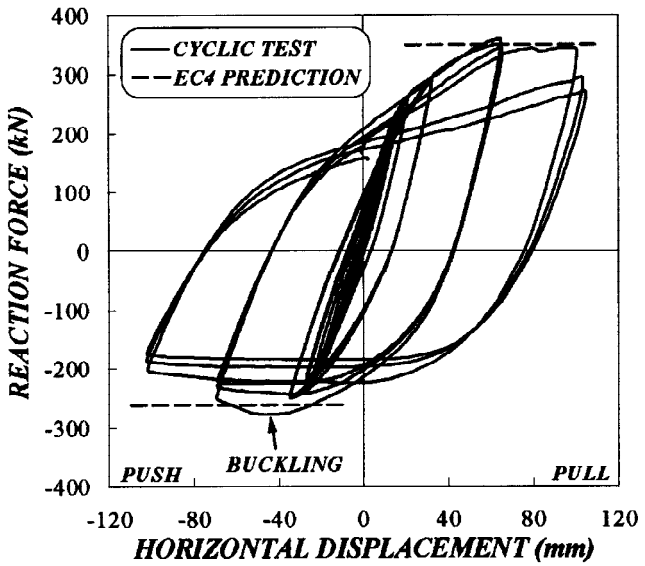

Fig. 4. Hysteresis loops of reaction force vs. controlled displacement of beam with full shear connection.

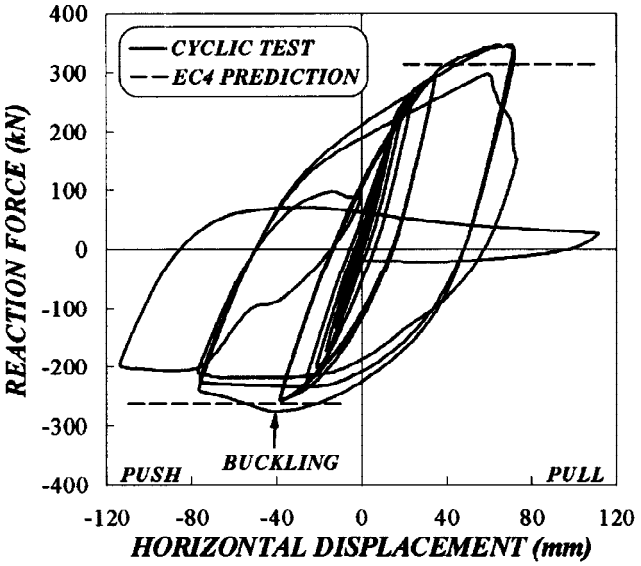

Fig. 5. Hysteresis loops of reaction force vs. controlled displacement of beam with partial shear connection.

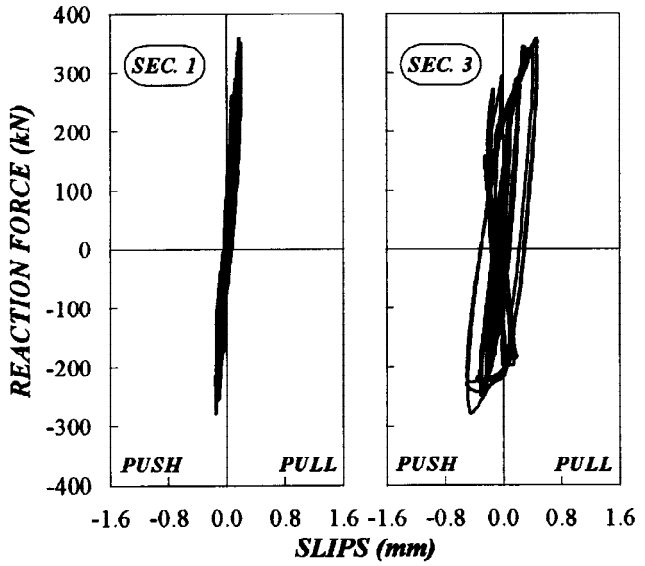

Fig. 6. Hysteresis loops of reaction force vs. 16 mm stud connector slips for beam with full shear connection.

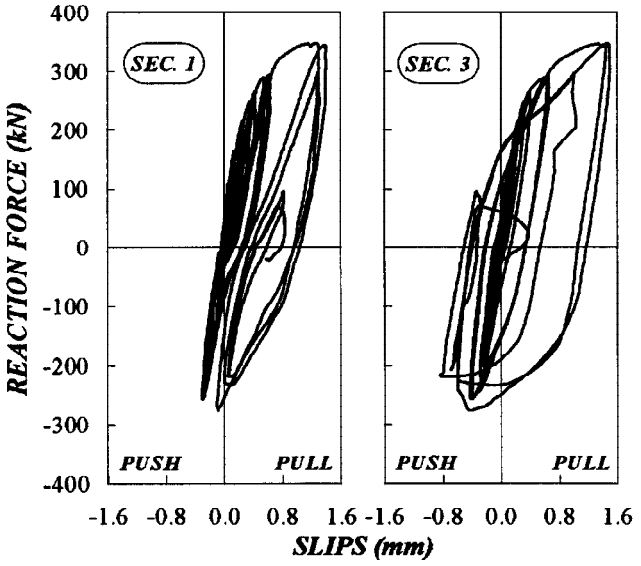

Fig. 7. Hysteresis loops of reaction force vs. 16 mm stud connector slips for beam with partial shear connection.

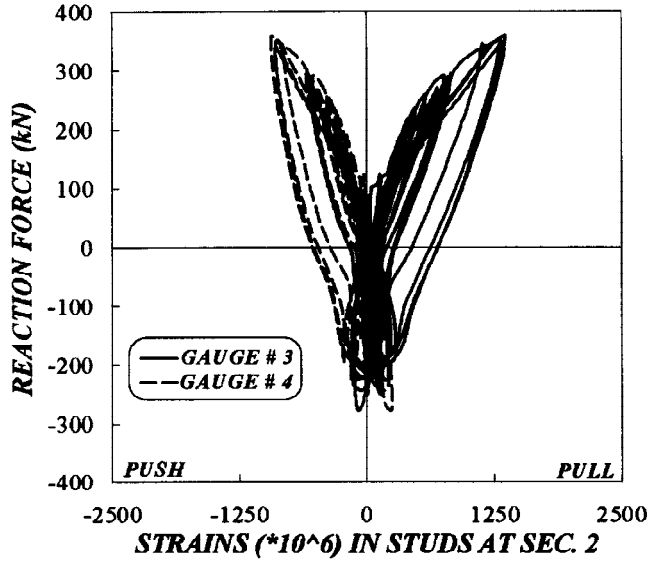

Fig. 8. Hysteresis loops of reaction force vs. stud strains at Sec. 2 for beam with full shear connection.

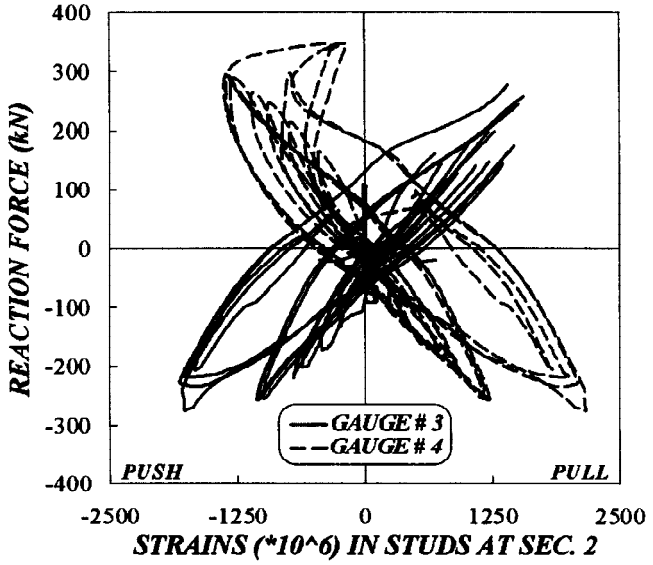

Fig. 9. Hysteresis loops of reaction force vs. stud strains at Sec. 2 for beam with partial shear connection.

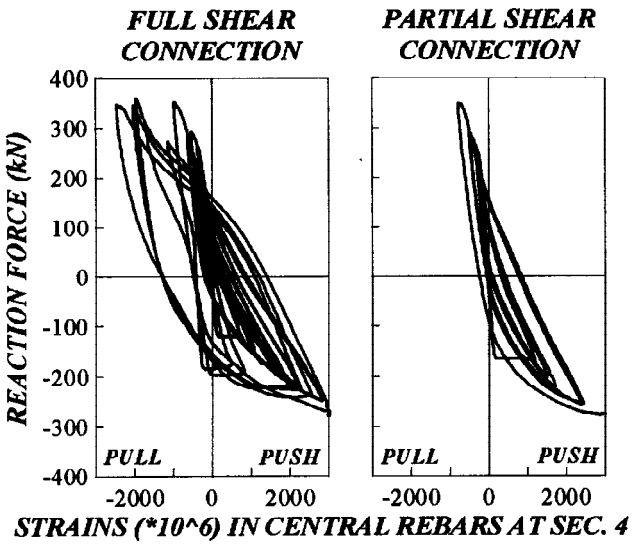

Fig. 10. Hysteresis loops of reaction force vs. measured strains in central rebars at Sec. 4.

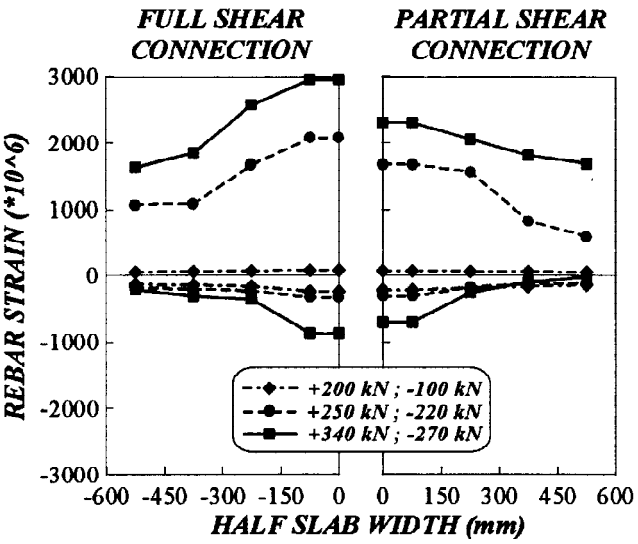

Fig. 11. Measured rebar strain in Sec. 4 at significant load levels.

Table 1. Stiffness and strength properties of beam response envelopes

	FULL SHEAR CONNECTION	*PARTIAL SHEAR CONNECTION*
K_0^+ (kN/mm)	16.7	14.6
F_p^+ (kN)	252.0	248.0
K_h^+ (kN/mm)	2.4	2.9
K_0^- (kN/mm)	12.2	12.2
F_p^- (kN)	228.2	212.9
K_h^- (kN/mm)	7.8	9.5

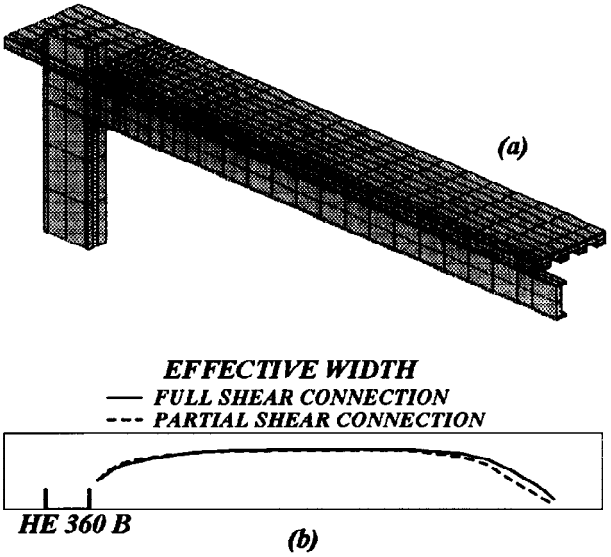

Fig. 12. Composite beams: (a) three-dimensional FE mesh; (b) effective width of slabs.

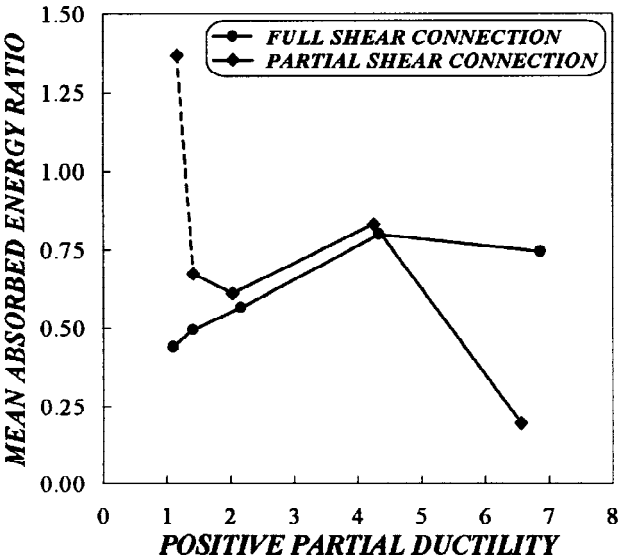

Fig. 13. Mean absorbed energy ratio in positive hemi-cycles vs. positive partial ductility.

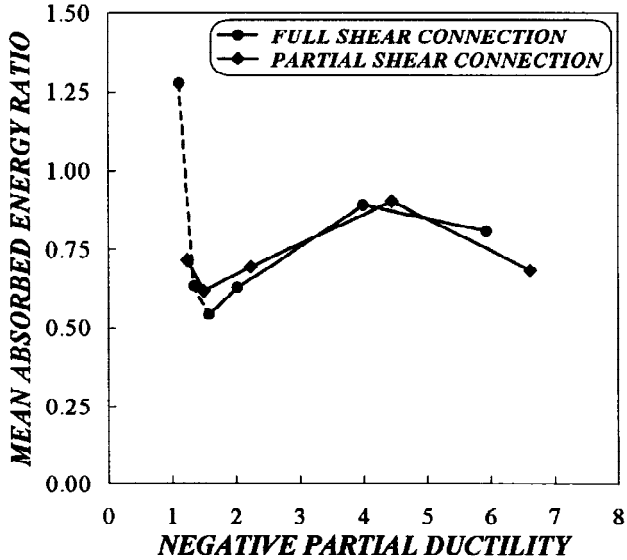

Fig. 14. Mean absorbed energy ratio in negative hemi-cycles vs. negative partial ductility.

The reaction forces of the FSC and PSC beams against the averaged slip measurements detected at Sec. 1 and 3 (see Fig. 1a) are illustrated in Figs. 6 and 7, respectively. One can observe that concrete slab-top flange interface slip is developed also in the FSC specimen while a larger slip is provided by the PSC specimen.
An understanding of the stud connector stress state caused by cyclic loading can be obtained by means of strain gauges located in studs at Secs. 2 and 4 (see Fig. 1). The relevant graphs for studs at Sec. 2 are shown in Fig. 8 and 9 for the FSC and PSC specimen, respectively. Strain gauges 3 and 4 are located very close to the steel flange (see Fig. 1a), therefore they are expected to detect the highest strains. Based on stud material properties, one can observe that stud connectors of FCS beam exhibit an elastic behaviour while connectors embodied in PSC beam show an inelastic behaviour. However, strain measures of stud connectors at Sec. 4 (see Fig. 1) indicate also some inelastic phenomena for the FSC specimen. Due to concrete-rebar slip, only a qualitative understanding of the slab behaviour can be understood by looking at the rebar strain state. In Fig. 10, the hysteresis loops relevant to the central rebars (see Fig. 1b) are shown. From rebar material properties, one can observe how central rebars in both the FSC and the PSC beams experience yielding. However, rebar strains vary along the slab transversal direction due to the shear lag phenomenon. Its effect on the rebar strain state can be captured from the strain distribution shown in Fig. 11 and relevant to the Sec. 4. These strains correspond to significant reaction force levels, i.e. values within the elastic range (+200 kN, -100 kN), at the plastic failure regime (+250 kN, -220 kN) and close to the maximum reaction force level (+340 kN, -270 kN). One can observe that the rebar strain state appears to be more severe for the FSC beam. By means of an energy equivalence criterion, both a stiffness and a strength characterization of beam performances have been obtained through a piecewise-linear approximation of the specimen response envelopes shown in Figs. 4 and 5. The relevant values initial stiffness K_0, strain-hardening stiffness K_h and plastic failure load F_p for both positive and negative loads are collected in Table 1. From those data one can observe similar performances between the specimens. The graphs depicted in Fig. 11 show a remarkable effect of the shear lag phenomenon on the slab strain state. Hence, a composite beam model for two-dimensional (2D) frame analyses needs to embody a slab effective width. To this end, 3D finite element analyses were performed to quantify the relevant slab effective width, in the elastic regime. The finite element mesh and the computed effective widths are shown in Fig 12a and 12b, respectively. From Fig. 12b, one can observe that shear lag effects are significant and that only a slight width difference exists between the FSC and the PSC beam.
An additional comparison between the specimens can be obtained by plotting the mean absorbed energy ratio against the partial ductility ratio. Because hemicycles are not symmetrical, both the positive (see Fig. 13) and the negative displacement regime (look at Fig. 14) have been distinguished. For completeness, also hemicycles with $1 < e/e_y < 2$ and characterized by hysteresis phenomena are plotted. The relevant results indicate the good performances of specimens as well as the superiority of the PSC beam at significant ductility levels.

PULL-PUSH SPECIMENS

Usually, headed stud shear connectors are designed to resist static gravity loads in a steel-concrete composite beam. However during an earthquake, such connectors are subjected to reversed cyclic loading in order to distribute large horizontal inertial forces in slabs. Nevertheless, only a limited number of pull-push tests was performed in the United States (Hawkins and Mitchell, 1984, McMullin *et al.*, 1993). Hence, additional data are needed to be able to characterize the hysteretic behaviour of stud connectors.

Test Procedures and Results

In order to expand the experimental data base and to calibrate finite element models for concrete-stud connector interaction, four of eleven companion pull-push specimens have been tested according to the recommendations drafted by ECCS (1986). In particular, monotonic loading with some reversed cycle (specimen PM-01 and PM-02) as well as fully reversed cyclic loading (specimen PC-01 and PC-02) were applied to the specimens. The geometrical and mechanical characteristics of these specimens are identical to those of the composite beams, and follow the geometrical ratios established in EC-4 (1992) for specific push tests. The test specimens are shown schematically in Fig. 15. Measurement devices are constituted by LVDTs and strain gauges which allow the load-relative slip relationships as well as deformations of stud connectors to be detected. In detail, the push specimens PM and the specimen PC-01 embody 2 and 4 instrumented studs, respectively, while the specimen PC-02 is endowed with no strain gauge on studs. In addition, the relative slip e has been assumed as the prime parameter of test control.
The response envelopes of the total compression reaction force against the controlled mean slip e are shown in Fig. 16. One can observe the stiffness and strength reduction of the specimens subjected to fully reversed cyclic loads. In the same figure also the specimen shear resistance predicted by EC-4 is depicted, where distinct

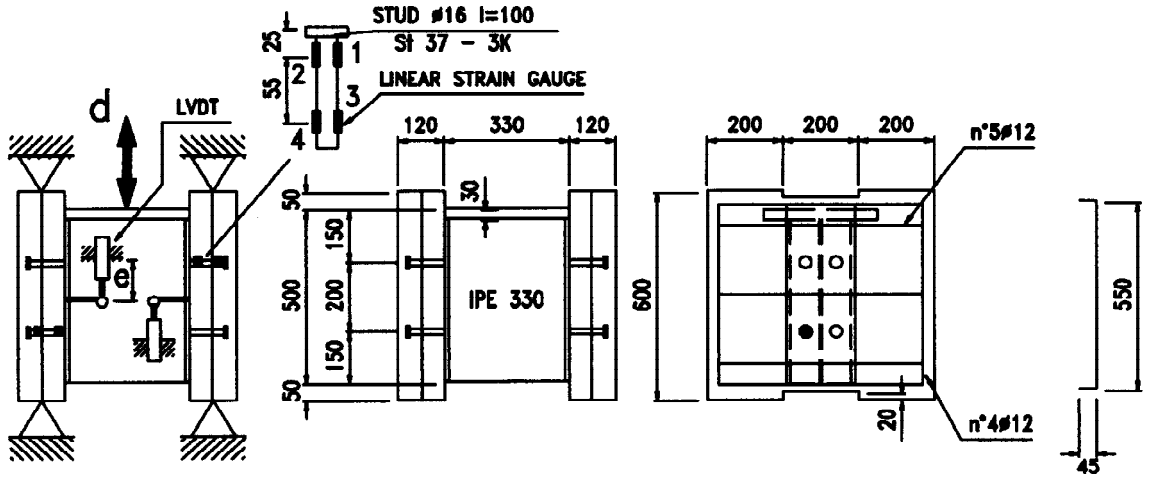

Fig. 15. Test pull-push characteristics and measurement apparatus.

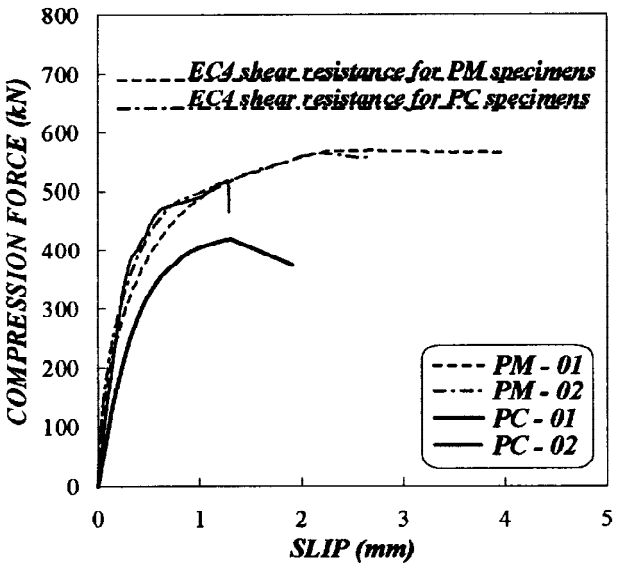

Fig. 16. Compression reaction force vs. controlled slip of pull-push specimens.

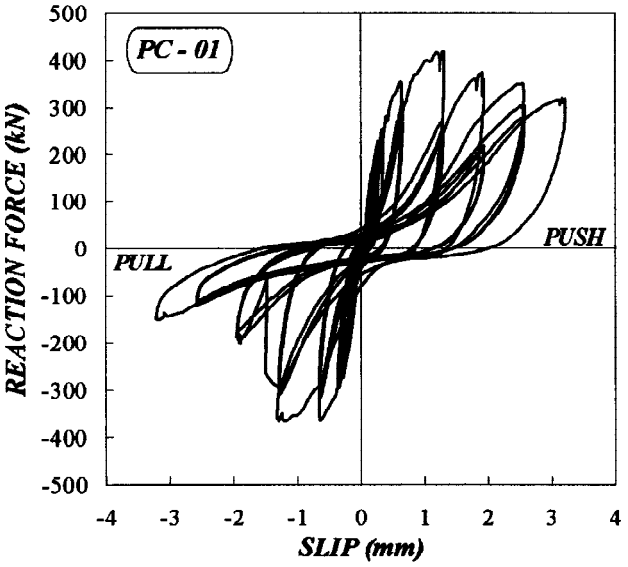

Fig. 17. Hysteresis loops of reaction force vs. controlled slip of pull-push specimen PC - 01.

Table 2. Stiffness and strength properties of compression pull-push response envelopes

	PUSH SPECIMENS		PULL-PUSH SPECIMENS	
	PM - 01	PM - 02	PC - 01	PC - 02
K_0^+ (kN/mm)	4716.0	4774.4	1284.0	2005.5
F_c^+ (kN)	109.0	114.0	111.0	111.0
K_r^+ (kN/mm)	658.7	805.7	517.8	1037.4
F_p^+ (kN)	485.0	466.0	374.0	435.0
K_h^+ (kN/mm)	40.4	59.2	62.8	91.5

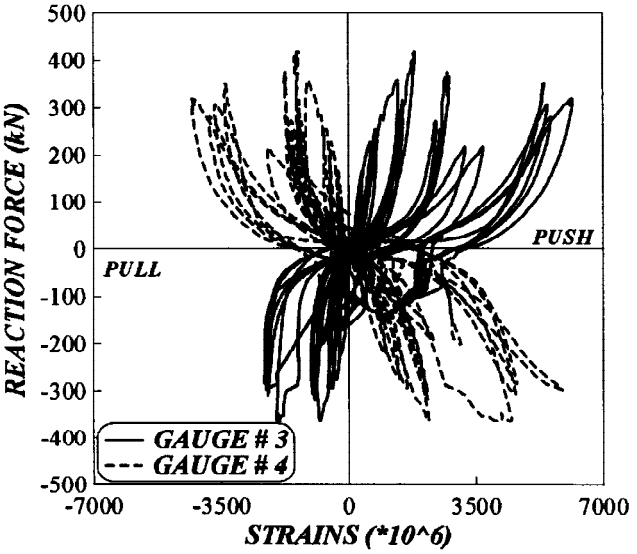

Fig. 18. Hysteresis loops of reaction force vs. stud connector strains of pull-push specimen PC - 01.

values correspond to different material properties. One can observe that the prediction is inaccurate due to the detrimental effects of cyclic loading on the specimen strength. The overall response of the PC-01 specimen is represented in Fig. 17. The observed inelastic behaviour is caused by stud connector yielding and concrete fracturing while the specimen collapse was governed by concrete crushing. In addition, due to damage effects, generally the first cycle required higher force and stiffness values than the corresponding values of the second and third cycle. The evaluation of the specimen performances can be obtained by means of Table 2, where the stiffness and strength properties of pull-push response envelopes under compression reaction forces are compared. In particular, the elastic stiffness K_0^+, the reduced stiffness K_r^+, the strain-hardening stiffness K_h^+, the cracking load F_c^+ and the plastic failure load F_p^+ are collected in the table. A reduced performance of the specimens PC-01 and PC-02 is evident. The strain state in stud connectors of specimen PC-01 can be assessed by means of the graph shown in Fig. 18. The strain state is relevant to gauges 3 and 4 (see Fig. 15) which are located very close to the beam flange. The strain levels indicate that stud connectors experience high inelastic deformations. In addition, the strain decomposition in axial and bending components allows both the tensile and bending generalized actions to be quantified. Finally, tests have shown that high curvatures develop at about 1.3 and 1.8 times the stud shank diameter from the stud base, with reference to the push and pull-push specimens, respectively.

CONCLUDING REMARKS

Quasi-static cyclic test results on composite beams with full and partial shear connection as well as complementary cyclic test data on pull-push specimens have been described. The preliminary test results on beam specimens are encouraging and verify that composite beams with discrete headed stud shear connectors and partial connection can perform satisfactorily in terms of strength, ductility and energy dissipation capability when ductile stud connectors can assure cyclic energy absorption, while splitting and pull-out of concrete can be prevented. In addition, it has been shown that shear lag effects are significant in composite slabs and that they need to be embodied in composite beam models in order to perform two-dimensional frame analyses. Furthermore, complementary tests on pull-push specimens highlighted severe stiffness and strength degradation phenomena due to reversed load cycles. Finally, actual design predictions calibrated upon monotonic loading appear to be unsatisfactory for the aforementioned test results.

ACKNOWLEDGEMENTS

This research project is sponsored by grants from C.N.R. and M.U.R.S.T. of Italy for which the authors are grateful. The skillful work of R. Battocletti, G. Gramola and the technical staff of the Testing Laboratory is greatly appreciated. The findings, observations and conclusions are, however, those of the writers.

REFERENCES

Bouwkamp J.G. and E. Fehling (1992). Comparison of r/c and composite frames for earthquake resistant design. In: *Proc. 10th World Conf. on Earth. Eng.*, Vol. 6, pp 3455-3460. Balkema, Rotterdam.

European Committee for Standardization (1992). *Eurocode 4, Design of Composite Steel and Concrete Structures - Part 1-1: General rules and rules for buildings*, ENV 1994-1-1.

Hawkins, N. and D. Mitchell (1984). Seismic response of composite shear connections. *J. of Struct. Eng., ASCE*, 110, 2120-2136.

Kim, W. and Lu, L.W. (1994). Hysteretic analysis and modeling of composite beam-columns. In: *Proc. 5th U.S. Nat. Conf. on Earth. Eng.*, (EERI ed.), Vol. 1, pp 273-282. EERI, California.

McMullin, K.M., A. Astaneh-Asl, G.L. Fenves and E. Fukuzava (1993). *Innovative semi-rigid steel frames for control of the seismic response of buildings*, Report No. UCB/EERC-93/03, California.

Shing, P.B., M. T. Vannan and E. Carter. (1991). Implicit time integration for pseudodynamic tests. *Earthquake Eng. Struct. Dyn.*, 20, 551-576.

Technical Committee 13 (1986). *Recommended testing procedure for assessing the behaviour of structural steel elements under cyclic loads.* (ECCS ed.), N. 45.